PHYSICAL REVIEW D **80,** 094002 (2009)

$W + 3$ jet production at the Tevatron

R. Keith Ellis*
Fermilab, Batavia, Illinois 60510, USA

Kirill Melnikov†
Department of Physics and Astronomy, Johns Hopkins University, Baltimore, Maryland, USA

Giulia Zanderighi‡
Rudolf Peierls Centre for Theoretical Physics, 1 Keble Road, University of Oxford, UK
(Received 18 June 2009; published 4 November 2009)

We compute the next-to-leading order QCD corrections to the production of W bosons in association with three jets at the Tevatron in the leading color approximation, which we define by considering the number of colors and the number of light flavors as being of the same order of magnitude. The theoretical uncertainty in the next-to-leading order prediction for the cross section is of the order of 15%–25% which is a significant improvement compared to the leading order result.

DOI: 10.1103/PhysRevD.80.094002 PACS numbers: 12.38.Bx

I. INTRODUCTION

Production of Z and W bosons in association with jets is an important process in hadron collider physics [1]. Indeed, the inclusive production cross section provides valuable information about fundamental parameters of the standard model as well as parton distribution functions. When the inclusive cross section is split into components depending on the number of jets, different $V + n$ jet samples ($V = W$, Z) become backgrounds to a variety of processes that include top pair production, single top production, Higgs boson production, and many other processes that might appear in extensions of the standard model. To understand these backgrounds, careful studies of vector boson production in association with jets were performed at the Tevatron by the CDF and D0 collaborations [2–4].

The cross section for $V + n$ jet production depends on how jets are defined. For typical jet parameters employed by CDF and D0, the production cross sections for, say, $W^+(\to e^+\nu) + n$ jets range between about 30 picobarns for $n = 1$ and about half of a picobarn for $n = 3$. Given the few inverse femtobarns of luminosity collected at the Tevatron, detailed studies of these cross sections are possible. In fact, results on the $W +$ jets cross sections published by CDF several years ago were based on 320 pb^{-1} of data. It is expected that new analyses, based on about one inverse femtobarn of data, will appear soon.

Tevatron studies of vector boson production in association with jets [2,3] established proximity, to within a factor of 2, between theoretical predictions based on leading order (LO) matrix elements merged with parton showers, and experimental data. While a factor of 2 sounds like a significant discrepancy, we note that leading order computations of processes with a large number of partons always have uncertainties of this order because different choices of input parameters, such as the renormalization scale of the strong coupling constant or the factorization scale in parton distribution functions, lead to large changes. It is well known that this problem is significantly reduced if cross sections are computed through next-to-leading order (NLO) in the expansion in the strong coupling constant.

The CDF and D0 collaborations have compared their data with NLO QCD predictions [5] for $W + n$ jets and $Z + n$ jets, for $n \leq 2$. It turned out that NLO QCD describes data very well. This is very impressive given that NLO QCD predictions are essentially parameter-free since unphysical dependencies on renormalization and factorization scales are reduced to about 10%. This success of NLO QCD, combined with the importance of the $V +$ jets production process, suggests that extending NLO QCD predictions to higher-multiplicity processes may be the best way to describe vector boson production in association with jets reliably, both at the Tevatron and the LHC.

Unfortunately, extending NLO QCD computations to $V + 3$ and $V + 4$ jets is a difficult task for a number of reasons. For example, in the case of $V + 3$ jets, virtual one-loop amplitudes involve rank five six-point functions. Real emission corrections require an integration of the $V(\to l_1 l_2) + 6$ parton matrix elements squared over a six-particle phase-space; the complexity of such a computation approaches the current frontier for the description of multi-particle processes at tree level (see e.g. Ref. [6]). Clearly, the complexity of computations required to describe $V + 4$ jet production through NLO QCD is even higher.

In this paper we compute NLO QCD corrections to $W +$ 3 jet production at the Tevatron. We extend our previous computation of NLO QCD corrections to that process [7] by including all partonic channels, while working in the leading color approximation defined as $N_c \sim N_f \gg 1$,

*ellis@fnal.gov
†kirill@phys.hawaii.edu
‡g.zanderighi1@physics.ox.ac.uk

where $N_c = 3$ is the number of colors and $N_f = 5$ is the number of massless fermion flavors. We employ recently evaluated virtual one-loop amplitudes for $W + 5$ partons [8,9]. To compute real emission corrections we use the Catani-Seymour subtraction scheme suitably adapted to deal with the minimal set of color-ordered amplitudes [7]. We perform the computation within the framework of the MCFM parton level integrator [10].

Recently a computation of NLO QCD corrections to $W + 3$ jet production at the Tevatron was reported by Berger *et al.* [11]. That computation also uses leading color approximation although their definition of leading color differs from ours. In particular, the leading color approximation $N_c \gg N_f \gg 1$ is employed in Ref. [11] only in the finite parts of virtual corrections, while real emission corrections are computed with full N_c and N_f dependence. We also note that preliminary results for *full color* NLO QCD corrections to $W + 3$ jets were presented recently [12]. Because the computation that we report here is strictly leading color, it is less accurate than results reported in [12]. Nevertheless, we believe that our results are worthwhile for two reasons. First, as we will see, the leading color approximation is sufficiently accurate for the phenomenology of $W + 3$ jets production given the size of experimental errors. Second, independent cross checks of these very challenging computations are important.

The remainder of this paper is organized as follows. In Sec. II we present a short summary of theoretical methods employed in the computation and describe details of the experimental measurement relevant for a comparison with theory. In Sec. III we present the results of our computation of $W + 3$ jet process at the Tevatron at leading and next-to-leading order. We conclude in Sec. IV.

II. SETUP OF THE CALCULATION

A. Theoretical set up

Our goal is to compute the $W + 3$ jet production cross section through next-to-leading order in perturbative QCD in the leading color approximation. We define this approximation as follows. We consider the limit $N_c \sim N_f \gg 1$, where N_c is the number of colors, N_f is the number of massless flavors, and we drop terms that are subleading in N_c. We keep all terms $\mathcal{O}(N_f/N_c)$. This has the consequence that both fermion loops in virtual corrections and processes with fermion pairs in the final state are retained. Fermion loops contribute to the running of the coupling, which is responsible for large scale variations of the leading order cross section (see below). Since, for $N_f = 5$, fermion contributions reduce the QCD beta function by about 20%, fermion loops may be important numerically. Once the $N_c \sim N_f \gg 1$ approximation is adopted, all partonic channels that contribute to hadron-hadron collisions need to be considered.

Any NLO QCD computation requires three ingredients—one needs to compute one-loop virtual corrections to the relevant leading order process, real emission corrections, and subtraction terms. Many issues related to dealing with these three ingredients are standard, at least as a matter of principle. In practice, for $W + 3$ jet production, the required one-loop and tree-level computations approach a degree of complexity where standard tools may not work efficiently. For example, there are of the order of 1500 one-loop diagrams that contribute to $W + 5$ parton scattering amplitudes. These diagrams involve rank five six-point functions which are the current frontier in one-loop computations.[1]

Real emission corrections require computations of complexity similar to $W + 4$ jets at tree level. Although no loops are involved in the latter case, this computation is very challenging because of the effort required to compute the relevant matrix elements and to integrate them over high-multiplicity phase space of the final state particles. In the next few paragraphs we describe some ideas that we used to overcome these difficulties.

Our computation of one-loop virtual amplitudes for $W + 3$ jets employs a particular technique called generalized D-dimensional unitarity [14]. It is one of several approaches pursued currently [15–17] which are based on a connection between one-loop scattering amplitudes and tree-level amplitudes for complex on- shell momenta [18–21]. All amplitudes required for the $W + 3$ jets computation are described in Ref. [9].

Our treatment of the real emission corrections is based on the Catani-Seymour dipole subtraction formalism [22]. However, some modifications of the formalism are required in our case since we deal with leading color amplitudes and extensively use symmetry of the final state phase space to reduce the number of color-ordered amplitudes that need to be calculated. Modifications of the subtraction formalism as well as issues related to our treatment of multiparticle phase space are discussed in Ref. [7].

Because we employ the leading color approximation, it is important to discuss its accuracy. We may get an idea about the quality of the leading color approximation by studying $W + 3$ jets at leading order and $W + n$ jets, $n \leq 2$, at next-to-leading order.

We find that for $W + 3$ jet at leading order, the leading color cross-section exceeds full color cross sections by about 10%. This result holds for various observables and

[1]We note that recently the complete calculation of NLO QCD corrections to $PP \to t\bar{t}b\bar{b}$ was performed with techniques that rely on Feynman diagrams and numerical reduction of one-loop tensor integrals [13]. That calculation also involves a comparable number of diagrams, however the tensor structure is simpler (it involves only up to rank four hexagons) and the number of subprocesses to be considered is considerably reduced. Nevertheless, the performance of the code used in that calculation is impressive both in terms of speed and stability.

is independent of the choice of the renormalization and factorization scales. In particular, the constant rescaling is valid bin-by-bin for the distributions considered here. This independence suggests that rescaling the leading color production cross section by a constant factor will lead to an improved estimate of the cross section beyond leading order. Therefore, we define our best approximation to a generic observable $\mathcal{O}$ computed through NLO QCD as

$$\frac{d\sigma^{\mathrm{NLO}}_{W+3\mathrm{jet}}}{d\mathcal{O}} = \mathcal{R}\int d\sigma^{\mathrm{NLO,LC}}_{W+3\mathrm{jet}}\,\delta(\mathcal{O}(p) - \mathcal{O}),$$
$$\mathcal{R} = \frac{\sigma^{\mathrm{LO,FC}}_{W+3\mathrm{jet}}}{\sigma^{\mathrm{LO,LC}}_{W+3\mathrm{jet}}}. \tag{1}$$

We call this procedure ''leading color adjustment''.

The major effect of this procedure on the leading color cross section is to rescale the leading order term in Eq. (1) making it the exact leading order full color result. A similar rescaling of the next-to-leading order correction in Eq. (1) is more questionable. Nevertheless, as long as the next-to-leading order correction is not excessively large, this procedure should provide a sensible approximation to the full color next-to-leading order result.

We can check this assertion by applying the leading color adjustment procedure to $W + 1$ and $W + 2$ jet NLO production cross sections. In both cases we find that rescaled leading color cross sections agree with full color cross sections to better than 3%.

B. Theoretical parameters and implementation of experimental cuts

The goal of this section is to describe precisely what we compute theoretically and its relationship to the measurement by the CDF collaboration. We consider the production of *on shell* $W^{\pm}$ bosons, that decay into a pair of massless leptons. We note that finite width effects are about 1% and that considering on shell production tends to *overestimate* the cross section. We set the Cabibbo-Kobayashi-Maskawa matrix to the identity matrix; this *reduces* the $W + 3$ jet production cross section at the Tevatron by about 1%. All quarks, with the exception of the top quark, are considered massless. The top quark is considered infinitely heavy and its contribution is neglected. The mass of the W is taken to be $m_W = 80.419$ GeV. W couplings to fermions are obtained from $\alpha_{\mathrm{QED}}(m_Z) = 1/128.802$ and $\sin^2\theta_W = 0.230$. We use CTEQ6L parton distribution functions for leading order and CTEQ6M for next-to-leading order computations [23,24] corresponding to $\alpha_s(M_Z) = 0.130$ and $\alpha_s(M_Z) = 0.118$, respectively. We quote results for three (dynamical) renormalization and factorization scales $\mu = [\mu_0/2, \mu_0, 2\mu_0]$, where $\mu_0 = \sqrt{p^2_{\perp,W} + m^2_W}$ and $p_{\perp,W}$ is the transverse momentum of the W boson. We choose these input parameters to stay maximally close to the choices made in Ref. [11] in order to facilitate a comparison between the two results, to the extent possible.

In the following we present results for the cuts employed in the analysis by the CDF collaboration [2]. We require that the transverse energy and pseudorapidity of the jets satisfy $E_{\perp,j} > 20$ GeV and $|\eta_j| < 2$ and employ the following restrictions on lepton transverse momentum, missing transverse energy, lepton rapidity, and transverse invariant mass $p^e_{\perp} > 20$ GeV, $\not{E}_{\perp} > 30$ GeV, $|\eta_e| < 1.1$, $M^W_{\perp} > 20$ GeV. We do not apply an isolation cut on the leptons since it is removed by the acceptance correction applied to the experimental results.

To define jets, the CDF collaboration uses the JETCLU cone algorithm with $R = 0.4$ and merging parameter $f = 0.75$. Since this algorithm is not infrared safe, it can not be used in a next-to-leading order calculation of $W + 3$ jets. As discussed in the next section, for the computations reported in this paper we choose to use a somewhat related but infrared safe seedless cone (SIScone) algorithm [25] and the anti-$k_{\perp}$ jet algorithm [26].

III. LEADING ORDER RESULTS

In this section, we summarize leading order results for total cross sections. We note that there is a subtlety associated with the way CDF presents their results. While jets are required to have transverse energy in excess of 20 GeV, the total cross section for $W + 3$ jet production is quoted with an *additional restriction*—the transverse energy of the third hardest jet should satisfy $E^{3\mathrm{rd\ jet}}_{\perp} > 25$ GeV. The CDF measurement yields the inclusive cross section

$$\sigma^{W+\geq 3j}_{E^{3\mathrm{rd\ jet}}_{\perp} > 25\ \mathrm{GeV}} = (0.84 \pm 0.10(\mathrm{stat}) \pm 0.21(\mathrm{sys}) \pm 0.05(\mathrm{lum}))\ \mathrm{pb}. \tag{2}$$

Note that this result includes both $W^+(e^+\nu)$ and $W^-(e^-\bar{\nu})$ production which, given the charge symmetry of the initial state at the Tevatron, simply doubles the cross section for fixed W charge.

We now discuss the choice of the jet algorithm in more detail. As we already mentioned, the CDF collaboration uses the infrared unsafe JETCLU jet algorithm. We remind the reader that infrared unsafety arises because one searches for stable cones around few fixed points (seeds) in the $\eta - \phi$ plane and one might miss a stable cone. It is often argued [27] that this is mainly an issue of perturbative calculations, which involve only few particles, and therefore few seeds. In a true experimental environment, with many soft emissions giving rise to many seeds, stable cones are rarely missed and the difference between infrared safe and unsafe jet algorithms is claimed to be small [27].

However, even if such claims are true, our inability to use infrared unsafe jet algorithms in theoretical computations makes it necessary to choose a jet algorithm which on one hand is infrared safe and, on the other hand, is close to

TABLE I. Leading order cross sections in picobarns for $W + 3$ jets at the Tevatron for different jet algorithms. We use merging parameter $f = 0.75$ for JETCLU and $f = 0.5$ for SISCone. The renormalization and factorization scales are set to μ_0. The upper (lower) value corresponds to setting both scales to $\mu_0/2$ and $2\mu_0$, respectively. Statistical errors are also indicated. Other cuts on jets and leptons are described in the text.

Algorithm	R	$E_\perp^{\text{jet}} > 20$ GeV	$E_\perp^{\text{3rd jet}} > 25$ GeV
JETCLU	0.4	$1.845(2)^{+1.101(3)}_{-0.634(2)}$	$1.008(1)^{+0.614(2)}_{-0.352(1)}$
SIScone	0.4	$1.470(1)^{+0.765(1)}_{-0.560(1)}$	$0.805(1)^{+0.493(1)}_{-0.281(1)}$
Anti-$k_\perp$	0.4	$1.850(1)^{+1.105(1)}_{-0.638(1)}$	$1.010(1)^{+0.619(1)}_{-0.351(1)}$

JETCLU in phenomenological applications. To facilitate such a choice, in Table I we compare leading order results for $W + 3$ jet production cross sections for two different jet algorithms, SISCone and anti-$k_\perp$. We observe that different jet algorithms for identical values of R lead to different results–not an unexpected conclusion.

If we consider jet algorithms for fixed value of $R = 0.4$, we find that anti-$k_\perp$ jet algorithm provides results that are closest to JETCLU. The SIScone algorithm does not do particularly well—the difference between SIScone and JETCLU with the same R is about 20%. Perturbative studies of jet substructure [28] suggest that the jet algorithm closest to CDF's JETCLU jet algorithm is anti-$k_\perp$. Therefore, it appears that anti-$k_\perp$ algorithm should be chosen for our calculation of $W + 3$ jet production cross section at the Tevatron.

The caveat in this discussion is that since JETCLU is not an infrared safe algorithm, the significance of leading order comparisons is unclear since radiative corrections can be arbitrarily large. Hence, it is not obvious that the most appropriate jet algorithm for theoretical calculations is the one which matches the JETCLU leading order results. To study this question, we perform the next-to-leading order calculation using both SIScone algorithm with $R = 0.4$ and $f = 0.5$ and the anti-$k_\perp$ algorithm with $R = 0.4$. The NLO computation with the SIScone algorithm allows us to compare our results to that of Ref. [11]. A similar computation with the anti-$k_\perp$ algorithm, would, if we had perfect data, tell us whether the agreement at leading order between JETCLU and anti-$k_\perp$ is fortuitous.

We now summarize the leading order results for the two algorithms. Using the three choices of the renormalization and factorization scales discussed previously, to set upper and lower bounds on the cross -section variation, we obtain the following result for leading-color and full-color leading order cross-sections:

$$\begin{aligned}\sigma^{W+\geq 3j,\text{LC}}_{\text{LO},E_\perp^{\text{3rd jet}}>25\ \text{GeV}} &= 0.89^{+0.55}_{-0.31}\ \text{pb},\\ \sigma^{W+\geq 3j,\text{FC}}_{\text{LO},E_\perp^{\text{3rd jet}}>25\ \text{GeV}} &= 0.81^{+0.50}_{-0.28}\ \text{pb}, \qquad \text{SIScone};\end{aligned} \tag{3}$$

$$\begin{aligned}\sigma^{W+\geq 3j,\text{LC}}_{\text{LO},E_\perp^{\text{3rd jet}}>25\ \text{GeV}} &= 1.12^{+0.68}_{-0.39}\ \text{pb},\\ \sigma^{W+\geq 3j,\text{FC}}_{\text{LO},E_\perp^{\text{3rd jet}}>25\ \text{GeV}} &= 1.01^{+0.62}_{-0.35}\ \text{pb}, \qquad \text{anti-}k_\perp.\end{aligned} \tag{4}$$

In Eqs. (3) and (4), central values are for the scale μ_0 and upper (lower) values are for $\mu_0/2$ and $2\mu_0$, respectively. We remind the reader that CTEQ6L parton distribution functions are used in leading order calculations.

The following comments can be made about Eqs. (3) and (4). First, as pointed out in the previous section, full color results are lower than the leading color results by about 10%; because of that, we will use $\mathcal{R} = 0.91$ for both algorithms to rescale NLO leading color calculations. Second, it is apparent from Eqs. (3) and (4) that, in spite of using a dynamical scale in the leading order computation, the scale variation of the leading order cross section is large. We can quantify it by introducing the following ratio $\xi^i = \sigma^i(\mu_{\max})/\sigma^i(\mu_{\min})$, where $i = \text{LO, NLO}$ defines the order at which the cross section is computed, and $\mu_{\max,\min}$ are the scales which give the largest (smallest) cross section for the three scales considered. We obtain $\xi^{\text{LO}} \approx 2.5$. for both SIScone and anti-$k_\perp$ algorithms. Note that while precise value of ξ is cut-dependent, the quoted result is typical—large variations of the cross section come from a strong dependence on the renormalization scale, due to the fact that the cross section depends on the third power of the strong coupling constant, $\sigma^{W+3j} \sim \alpha_s^3$.

IV. NEXT-TO-LEADING ORDER RESULTS

In this section, we summarize the next-to-leading order results. Working in the leading color approximation, we obtain the inclusive jet cross section[2]

$$\sigma^{W+\geq 3j,\text{LC}}_{\text{NLO},E_\perp^{\text{3rd jet}}>25\ \text{GeV}} = 1.01^{+0.05}_{-0.17}\ \text{pb}, \qquad \text{SIScone}, \tag{5}$$

$$\sigma^{W+\geq 3j,\text{LC}}_{\text{NLO},E_\perp^{\text{3rd jet}}>25\ \text{GeV}} = 1.10^{+0.01}_{-0.13}\ \text{pb}, \qquad \text{anti-}k_\perp. \tag{6}$$

Scaling these results by the tree-level ratio of full color and leading color leading order cross sections, $\mathcal{R}$, as explained in the previous section, we obtain

$$\sigma^{W+\geq 3j}_{\text{NLO},E_\perp^{\text{3rd jet}}>25\ \text{GeV}} = 0.91^{+0.05}_{-0.15}\ \text{pb}, \qquad \text{SIScone}, \tag{7}$$

$$\sigma^{W+\geq 3j}_{\text{NLO},E_\perp^{\text{3rd jet}}>25\ \text{GeV}} = 1.00^{+0.01}_{-0.12}\ \text{pb}, \qquad \text{anti-}k_\perp. \tag{8}$$

The next-to-leading computation shows a significant improvement in stability with respect to changes in the

[2]In the case of anti-$k_\perp$, the central value quoted corresponds to a scale $\mu = \mu_0/2$, while the upper (lower) bounds correspond to $\mu = \mu_0$ and $\mu = 2\mu_0$, respectively.

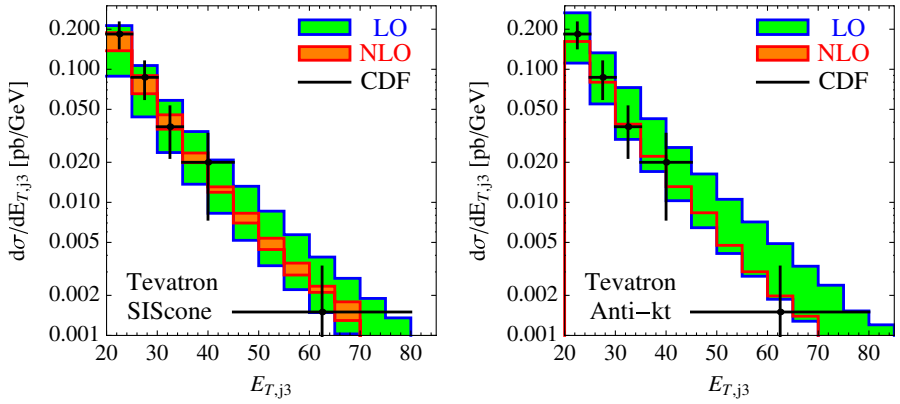

FIG. 1 (color online). The transverse energy distribution of the third hardest jet for $W + 3$ jet inclusive production cross section at the Tevatron for SIScone (left) and anti-$k_\perp$ (right) jet algorithms. All cuts and parameters relevant for deriving these distributions are described in the text. The leading color adjustment procedure is applied. For experimental points, statistical and systematic uncertainties are combined in quadrature. The bands illustrate the scale dependence at leading (green) and next-to-leading order (red).

renormalization and factorization scales. Calculating the parameter ξ, introduced in the previous section, we find $\xi^{\rm NLO}_{\rm SIScone} = 1.25$ and $\xi^{\rm NLO}_{\text{anti-}k_\perp} = 1.15$ which implies that *overall* uncertainty in the NLO QCD prediction is 25% or better. Compared to leading order predictions, the uncertainty is reduced by at least a factor of 4.

We also find that the difference between NLO cross sections computed with SIScone and anti-$k_\perp$ is smaller than the difference between corresponding leading order cross sections. Nevertheless, the difference at NLO is about 10% and therefore it will not be negligible when high precision data will become available. Currently, experimental data seems to be closer to SIScone; however, given a 20% uncertainty in data and up to 20% uncertainty in the NLO results, no inconsistency can be claimed.

CDF published the transverse energy distribution of the third hardest jet in $W + 3$ jet inclusive production cross section. In Fig. 1, we compare the theoretical prediction for this distribution at leading and next-to-leading order with experimental data for the two jet algorithms. For experimental points, statistical and systematic uncertainties are combined in quadrature. Theoretical results are rescaled by $\mathcal{R} = 0.91$ bin-by-bin, following the discussion in Sec. II. There is reasonable agreement with data, although uncertainties in current data do not permit high-precision comparison.

It is interesting to observe that shapes of transverse energy distributions differ at LO and NLO. Comparing distributions evaluated at a common scale μ_0, the NLO result exceeds the leading order cross section at low values of the third jet transverse energy $E_\perp^{\rm 3rd}$ and is below the leading order cross section for higher values of $E_\perp^{\rm 3rd}$. Such behavior is consistent with the expectation that emission of additional QCD partons is governed by the strong coupling constant evaluated at the transverse momentum of a ''daughter parton'' defined relative to the direction of a ''parent parton'' in a QCD branching. When the third hardest jet has small momentum, the scale $\mu_0 = \sqrt{p_{\perp,W}^2 + m_W^2}$ is larger than the relative transverse momentum in the branching that produced this jet; as the result, the leading order computation with the scale μ_0 underestimates the cross section. On the other hand, when the momentum of the third hardest jet increases, transverse momenta of the two leading jets start to exceed μ_0; as the result, the leading order computation with the scale μ_0 overestimates the cross section. The change of shape, therefore, can be attributed to an ''improper'' choice of the coupling constant renormalization scale in the leading order computation which gets naturally corrected once one-loop effects are included. Similar effects in $W + n$ jet production were recently discussed in Ref. [29] using soft-collinear effective theory.

It is instructive to study the relative importance of the various subprocesses and how the NLO corrections to them compare. The simplest way to split various contributions is into two-quark, four-quark, and six-quark subprocesses where the number of quarks is the *total* number of quarks in $W + 3$ jet amplitude (including those in the loop). The two-quark and four-quark processes give the largest contribution to the cross section while the six-quark processes not present at LO are relatively small ($\sim -7\%$). We find that NLO QCD corrections affect two-quark and four-quark processes differently—for example, at the reference scale μ_0 they increase the two-quark processes by about 50% while they decrease the four-quark processes by about 20%.

There are two lessons that we draw from this observation. First, it does not seem possible to determine optimal renormalization and factorization scales for the *whole* process by studying NLO QCD corrections to two- or four-quark processes *only*. Second, we observe that for the central scale $\mu = \mu_0$, NLO correction to the *total* cross section is rather modest—about 10%. However, this mod-

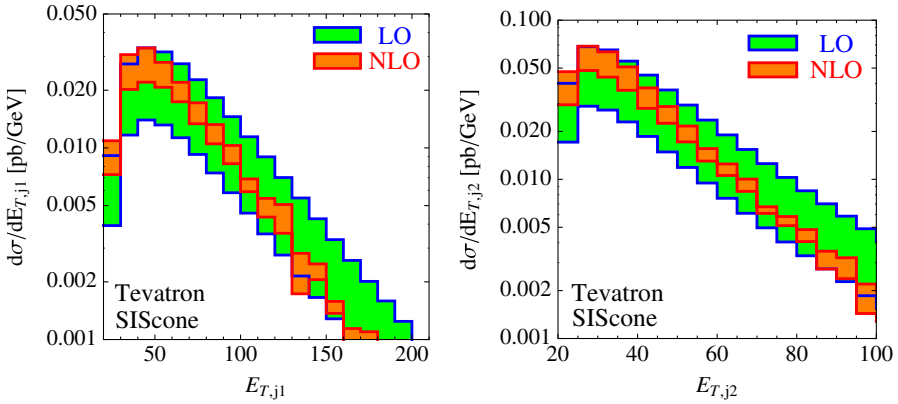

FIG. 2 (color online). The transverse energy distributions of the hardest (left) and second-to-hardest (right) jet in the $W + 3$ jet inclusive sample using SIScone jet algorithm. All cuts and parameters are described in the text. The leading color adjustment is applied. The bands illustrate the scale dependence at leading (green) and next-to-leading order (red).

est correction is the result of a cancellation between somewhat larger corrections to two-quark and four-quark channels. This suggests that the leading color adjustment procedure that we apply may not be very accurate since small corrections to the adjustment procedure for two- and four-quark channels *separately* may get amplified because of the cancellation. Note however that the systematic and luminosity errors on the $W + 3$ jet data are currently 25% and 6%, respectively [see Eq. (2)]. Given errors of this size, the leading color approximation seems sufficient for the foreseeable future.

In Figs. 2 and 3 we present other kinematic distributions computed through next-to-leading order. In Fig. 2, the transverse energy distributions of hardest and next-to-hardest jets are shown. These distributions exhibit a shape change similar to the shape change that we observed in the transverse momentum distribution of the third hardest jet.

In Fig. 3 the impact of NLO QCD corrections on leptonic observables in the case of $W^+ + \geq 3$ jet production is shown. In this case significant shape changes in both lepton rapidity distribution and missing energy distribution do not occur, so simulations based on leading order matrix elements should give reliable results for the shapes.

Finally, we point out that the discussion in this section applies to the *inclusive* $W + 3$ jets cross section. In particular, the observation that the choice of renormalization and factorization scale $\mu = \mu_0$ leads to small corrections applies to that observable. It is interesting to point out that the same scale choice $\mu = \mu_0$ also works very well for *exclusive* $W + 3$ jet production cross section. In that case, for $\mu = \mu_0$, the NLO QCD corrections increase the leading order result by only about 6%, if jets are defined with SIScone algorithm.

To conclude this section, we compare our findings with that of Berger *et al.* [11]. As we explained in the Introduction, the computation reported in this paper and in Ref. [11] are not identical so full agreement should not be expected. Nevertheless, the agreement is quite good. For example the leading color SIScone cross section $\sigma_{\rm NLO}^{W+\geq 3j}(E_\perp^{\rm 3rd\ jet} > 25\ {\rm GeV}) = 0.908^{+0.044}_{-0.142}$ pb was reported

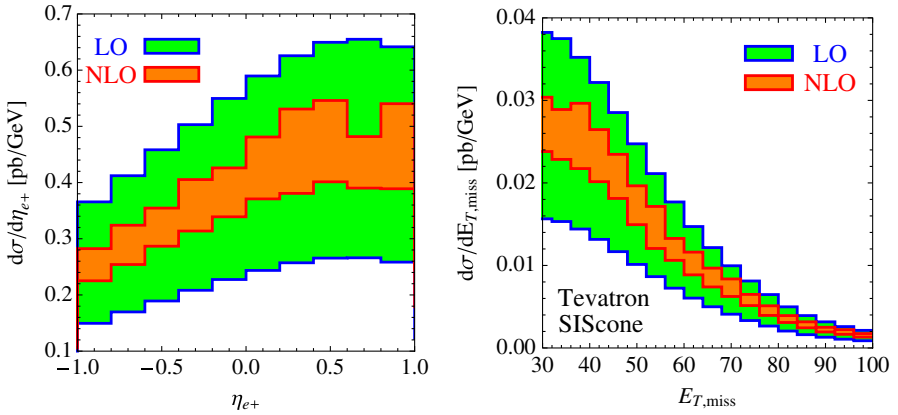

FIG. 3 (color online). The e^+ rapidity distribution and the missing energy distribution in the $W^+ + \geq 3$ jet sample using SIScone jet algorithm. All cuts and parameters are described in the text. The leading color adjustment is applied. The bands illustrate the scale dependence at leading (green) and next-to-leading order (red).

[11]. Based on the evidence from $W + 1$ and $W + 2$ jets, it was argued in [11] that their leading color cross section is within 3% of the full color result.[3] This result compares very well with our *estimate* of the full color result shown in Eq. (7).

V. CONCLUSIONS

We described the computation of NLO QCD radiative corrections to $W + 3$ jet cross section at the Tevatron, in the leading color approximation. We compared our results with experimental data and found agreement both for the total cross section and available differential distributions. We point out that the scale choice $\mu = \sqrt{p_{\perp,W}^2 + m_W^2}$ is fortunate at the Tevatron since for this dynamical scale QCD corrections to total cross sections are relatively small. On the other hand, this scale choice is not a perfect solution as evident from the fact that at NLO shapes of some distributions change.

Results presented here suggest that, after a leading color adjustment, leading color NLO calculations are an excellent approximation to the full color result, to within a few percent. This is more than enough to match the experimental accuracies of Tevatron and LHC measurements of multi-particle final state events. From a theoretical point of view, missing higher order next-to-next-to-leading order corrections, estimated through the residual scale dependence of the NLO result, limited knowledge of the underlying event, and poor description of hadronization effects give rise to much larger theoretical uncertainties than the error due to the adjusted leading color approximation.

[3]This claim is further supported by the preliminary full color NLO QCD cross section for $W + 3$ jets reported in [12].

Finally, we emphasize that for meaningful comparison of experimental and theoretical results, it is important to use identical jet algorithms. If this is not done, systematic differences between different jet algorithms at the level of 10% or larger can not be excluded and indeed do occur as follows from the comparison of NLO predictions for $W + 3$ jets obtained with SIScone and anti-$k_\perp$ algorithms. We point out that *any* jet algorithm can be used for a theoretical computation as long as it is infrared safe. Unfortunately, the JETCLU algorithm used by CDF in the published $W + 3$ jet analysis is not infrared safe and we had to switch to other jet algorithms. We found that NLO QCD prediction for $W + 3$ jets computed both with SIScone and anti-$k_\perp$ jet algorithms work reasonably well in that they show agreement with data within the quoted experimental and theoretical errors. It is important to stress, however, that it is much better to use identical infrared safe jet algorithms to avoid this issue in future comparisons.

ACKNOWLEDGMENTS

We are grateful to Carola Berger, Fernando Febres Cordero, and Zoltan Kunszt for useful discussions. G. Z. would like to thank, in particular, Lance Dixon for fruitful communication and exchange of information and Gavin Salam for extensive discussions about jet algorithms. We also thank John Campbell for providing the code needed to compute $W + 2$ jets in the leading color approximation. The research of K. M. is supported by the startup package provided by Johns Hopkins University. G. Z. is supported by the British Science and Technology Facilities Council. Fermilab is operated by Fermi Research Alliance, LLC under Contract No. DE-AC02-07CH11359 with the United States Department of Energy.

[1] For a review and earlier references, see e.g. P. Nadolsky, arXiv:hep-ph/0412146.
[2] T. Aaltonen *et al.* (CDF Collaboration), Phys. Rev. D **77**, 011108 (2008).
[3] T. Aaltonen *et al.* (CDF—Run II Collaboration), Phys. Rev. Lett. **100**, 102001 (2008).
[4] P. H. Nadolsky, AIP Conf. Proc. **753**, 158 (2005).
[5] J. Campbell and R. K. Ellis, Phys. Rev. D **65**, 113007 (2002).
[6] T. Gleisberg, S. Hoche, and F. Krauss, arXiv:0808.3672.
[7] R. K. Ellis, K. Melnikov, and G. Zanderighi, J. High Energy Phys. 04 (2009) 077.
[8] C. F. Berger *et al.*, arXiv:0808.0941.
[9] R. K. Ellis, W. T. Giele, Z. Kunszt, K. Melnikov, and G. Zanderighi, J. High Energy Phys. 01 (2009) 012.
[10] See http://mcfm.fnal.gov.
[11] C. F. Berger *et al.*, Phys. Rev. Lett. **102**, 222001 (2009).
[12] See talks by F. Cordero, D. Forde, and H. Ita, Loopfest conference, 2009 (unpublished).
[13] A. Bredenstein, A. Denner, S. Dittmaier, and S. Pozzorini, Phys. Rev. Lett. **103**, 012002 (2009).
[14] R. K. Ellis, W. T. Giele, and Z. Kunszt, J. High Energy Phys. 03 (2008) 003; W. T. Giele, Z. Kunszt, and K. Melnikov, J. High Energy Phys. 04 (2008) 049.
[15] G. Ossola, C. G. Papadopoulos, and R. Pittau, J. High Energy Phys. 03 (2008) 042.
[16] C. F. Berger *et al.*, Phys. Rev. D **78**, 036003 (2008).
[17] A. van Hameren, C. G. Papadopoulos, and R. Pittau, J. High Energy Phys. 09 (2009) 106 .
[18] Z. Bern, L. J. Dixon, D. C. Dunbar, and D. A. Kosower, Nucl. Phys **B425**, 217 (1994).
[19] Z. Bern, L. J. Dixon, D. C. Dunbar, and D. A. Kosower, Nucl. Phys. **B435**, 59 (1995).
[20] Z. Bern, L. J. Dixon, and D. A. Kosower, Nucl. Phys.

B513, 3 (1998).
[21] R. Britto, F. Cachazo, and B. Feng, Nucl. Phys. **B725**, 275 (2005).
[22] S. Catani and M. H. Seymour, Nucl. Phys. **B485**, 291 (1997); **B510**, 503(E) (1998).
[23] J. Pumplin, D. R. Stump, J. Huston, H. L. Lai, P. M. Nadolsky, and W. K. Tung, J. High Energy Phys. 07 (2002) 012.
[24] P. M. Nadolsky *et al.*, Phys. Rev. D **78**, 013004 (2008).
[25] G. P. Salam and G. Soyez, J. High Energy Phys. 05 (2007) 086.
[26] M. Cacciari, G. P. Salam, and G. Soyez, J. High Energy Phys. 04 (2008) 063.
[27] S. D. Ellis, J. Huston, K. Hatakeyama, P. Loch, and M. Tonnesmann, Prog. Part. Nucl. Phys. **60**, 484 (2008).
[28] G. P. Salam (private communication).
[29] C. W. Bauer and B. O. Lange, arXiv:0905.4739.